

Unconventional superconductivity in ζ -phase of oxygen compressed to megabar pressure

E. F. Talantsev^{1,2}

¹M.N. Miheev Institute of Metal Physics, Ural Branch, Russian Academy of Sciences,
18, S. Kovalevskoy St., Ekaterinburg, 620108, Russia

²NANOTECH Centre, Ural Federal University, 19 Mira St., Ekaterinburg, 620002,
Russia

E-mail: evgeny.talantsev@imp.uran.ru

Abstract

Oxygen exhibits structural phase transformation from non-metallic ε -O₂ phase into metallic ζ -O₂ phase at pressure of $P = 96$ GPa (Desgreniers *et al* 1990 *J. Phys. Chem.* **94** 1117; Akahama *et al* 1995 *Phys. Rev. Lett.* **74** 4690). Metallic ζ -O₂ phase is a superconductor with transition temperature of $T_c = 0.6$ K at $P = 115$ -120 GPa (Shimizu *et al* 1998 *Nature* **393** 767). In this paper we have performed analysis of temperature dependent upper critical field, $B_{c2}(T)$, for ζ -O₂ phase ($P = 115$ GPa) and show that this highly-compressed phase of gaseous molecular element is unconventional superconductor with the ratio of T_c to the Fermi temperature, T_F , in the range of $0.009 \leq T_c/T_F \leq 0.108$.

Unconventional superconductivity in ζ -phase of oxygen compressed to megabar pressure

I. Introduction

Jörg Wittig [1] heralded studies of pressure-induced superconductivity in non-superconductors by the discovery of superconducting transition in cerium with $T_c = 1.8$ K by applying isostatic pressure of $P = 5$ GPa. To date, the pressure-induced superconductivity has been detected in dozens of elements and compounds compressed at megabar pressures [2-18], including milestone experimental discoveries of near-room-temperature (NRT) superconducting hydrides [2-4,10-13].

Desgreniers *et al* [19] detected metallization of oxygen at pressures $P > 90$ GPa, and this phase transformation from non-metallic ε -O₂ phase into metallic ζ -O₂ phase has been studied for three decades [20-23].

Shimizu *et al* [8] reported that ζ -O₂ phase is a superconductor with transition temperature of $T_c = 0.6$ K at pressures in the range of $P = 115$ -120 GPa. Shimizu *et al* [8] also reported temperature dependent upper critical field data, $B_{c2}(T)$, which we analyse herein with the purpose to classify superconductivity (i.e., conventional vs unconventional) in ζ -O₂ phase.

Primary demand to perform this classification is based on our recent findings that all NRT highly-compressed superconductors are, surprisingly enough, unconventional superconductors [24-26], which exhibit the ratio of the superconducting transition temperature, T_c , to the Fermi temperature, T_F , in the range of $0.01 \lesssim \frac{T_c}{T_F} \lesssim 0.05$, which is the range for all known unconventional superconductors [27,28].

In result, we find that in all considered scenarios ζ -O₂ phase ($P = 115$ GPa) has T_c/T_F ratio in the range of $0.008 \lesssim \frac{T_c}{T_F} \lesssim 0.107$, and, thus, this highly-compressed phase of gaseous element should be classified as unconventional superconductor.

II. The upper critical field data analysis

Shimizu *et al* [8] in their Fig. 3 reported experimental $B_{c2}(T)$ data for ζ -O₂ phase at pressure $P = 115$ GPa which we fit to two models:

1. The first model was proposed by Baumgartner *et al* [29]:

$$B_{c2}(T) = \frac{\phi_0}{2 \cdot \pi \cdot \xi^2(0)} \cdot \left(\frac{\left(1 - \frac{T}{T_c}\right) - 0.153 \cdot \left(1 - \frac{T}{T_c}\right)^2 - 0.152 \cdot \left(1 - \frac{T}{T_c}\right)^4}{0.693} \right) \quad (1)$$

where $\phi_0 = 2.068 \cdot 10^{-15}$ Wb is magnetic flux quantum, and $\xi(0)$ is the ground state coherence length. We will designate this model as B-WHH model, because Eq.1 is analytical approximation of general model proposed by Werthamer, Helfand, and Hohenberg [30].

2. The second used model was proposed by Gor'kov [31]:

$$B_{c2}(T) = \frac{\phi_0}{2 \cdot \pi \cdot \xi^2(0)} \cdot \left(\frac{1.77 - 0.43 \cdot \left(\frac{T}{T_c}\right)^2 + 0.07 \cdot \left(\frac{T}{T_c}\right)^4}{1.77} \right) \cdot \left[1 - \left(\frac{T}{T_c}\right)^2 \right] \quad (2)$$

It should be noted, that both models (Eqs. 1,2) are in wide use at the moment to analyse experimental $B_{c2}(T)$ data for whole variety of superconducting materials, ranging from atomically thin superconductors [32] and practical superconductors [29] to NRT superconductors [24-26].

Results of fit of $B_{c2}(T)$ data for ζ -O₂ phase ($P = 115$ GPa) to Eqs. 1,2 are shown in Fig. 1 and deduced parameters are collected in Table 1.

Table I. Deduced and calculated parameters for ζ -O₂ phase compressed at pressure of $P = 115$ GPa. The smallest and the largest values for $\frac{T_c}{T_F}$ are marked in bold.

Model	Deduced T_c (K)	Deduced $\xi(0)$ (nm)	Assumed m_{eff}^* (in m_e)	Assumed $\frac{2 \cdot \Delta(0)}{k_B \cdot T_c}$	T_F (K)	T_c/T_F
B-WHH	0.635 ± 0.008	41.3 ± 0.4	0.49	3.53	5.86 ± 0.02	0.108 ± 0.003
				5.0	11.8 ± 0.02	0.052 ± 0.002
			3.0	3.53	35.9 ± 1.6	0.018 ± 0.001
				5.0	72.0 ± 3.2	0.009 ± 0.001
Gor'kov	0.63 ± 0.01	42.0 ± 0.7	0.49	3.53	5.96 ± 0.40	0.106 ± 0.005
				5.0	12.0 ± 0.02	0.053 ± 0.003
			3.0	3.53	36.5 ± 2.5	0.017 ± 0.001
				5.0	73.3 ± 4.8	0.009 ± 0.001

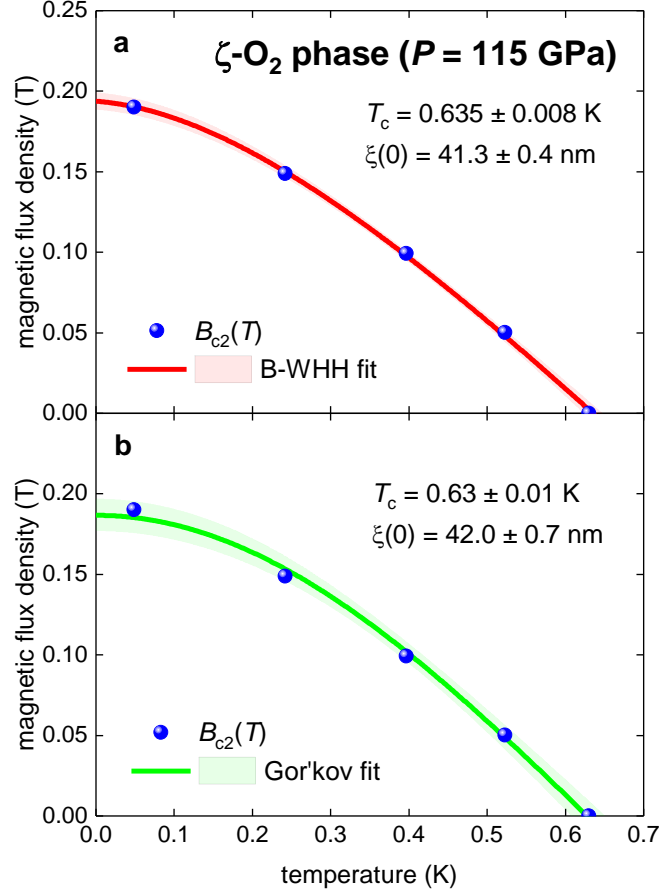


Figure 1. Superconducting upper critical field, $B_{c2}(T)$, data and fits to three models (Eqs. 1,2) for ζ -O₂ phase compressed at pressure of $P = 115$ GPa (raw data is from Ref. 8). (a) fit to B-WHH model, $R = 0.9994$; (b) fit to Gor'kov model, $R = 0.998$. 95% confidence bars are shown.

III. ζ -O₂ phase in Uemura plot

From known $\xi(0)$ and T_c values, the Fermi temperature, T_F , can be calculated by an equation of the Bardeen-Cooper-Schrieffer (BCS) theory [33]:

$$T_F = \frac{\varepsilon_F}{k_B} = \frac{\pi^2}{8} \cdot m_{eff}^* \cdot \xi^2(0) \cdot \left(\frac{\alpha \cdot k_B \cdot T_c}{\hbar} \right)^2, \quad (3)$$

where $\alpha = \frac{2 \cdot \Delta(0)}{k_B \cdot T_c}$, $\Delta(0)$ is the amplitude of the ground state energy gap, ε_F is the Fermi energy,

$\hbar = h/2\pi$ is reduced Planck constant, k_B is the Boltzmann constant, m_{eff}^* is the charge carrier effective mass.

As there are no available experimental $\alpha = \frac{2 \cdot \Delta(0)}{k_B \cdot T_c}$ and the effective charge carrier mass m_{eff}^* values for ζ -O₂ phase, to calculate T_F for ζ -O₂ phase we chose a reasonable lower and upper bounds for these values. For lower bound of m_{eff}^* we use the value for ambient pressure hydrogen-rich superconductor, PdH_x [34]:

$$m_{eff}^* = 0.49 \cdot m_e, \quad (4)$$

despite a fact that the closest (by T_c and by the atomic mass) ambient pressure superconductor to ζ -O₂ is the aluminium [35] with

$$m_{eff}^* = 1.0 \cdot m_e \quad (5)$$

In this regard, in lower bound for m_{eff}^* (Eq. 4) is chosen as intended underestimated value to cover some hypothetical case that m_{eff}^* might be reasonably low in ζ -O₂ phase. This lower bound for m_{eff}^* can be also supported by $m_{eff}^* = (0.2 - 0.5) \cdot m_e$ reported by Medvedeva [36] for multicomponent conducting oxides.

For the upper bound of m_{eff}^* we use the highest value reported for highly compressed hydrides, $m_{eff}^* = 3.0 \cdot m_e$ [37]. The possibility for heavy effective charge carrier mass in ζ -O₂, i.e. $m_{eff}^* > 3.0 \cdot m_e$, cannot be of course rejected a priori, but large effective masses, as a rule, always associated with strong interaction between spin and d - or f -orbitals, and the latter does not exist in such light elements, like oxygen. Thus, we do not consider a possibility that the effective mass can exceed mentioned above value of $m_{eff}^* = 3.0 \cdot m_e$.

The lowest value for $\frac{2 \cdot \Delta(0)}{k_B \cdot T_c}$ is weak-coupling limit of 3.53 [33], and for all known s -wave superconductors [38-40] α is limited by the upper bound of $\frac{2 \cdot \Delta(0)}{k_B \cdot T_c} \lesssim 5.0$ [38]. Thus, T_F is calculated (Table 1 and Fig. 2) in the assumption that α is varying within a range of $3.53 \leq \frac{2 \cdot \Delta(0)}{k_B \cdot T_c} \leq 5.0$ (it should be noted, that this range is cover most highly-compressed hydrogen-rich superconductors [24,37-42]).

As the result, ζ -O₂ phase ($P = 115$ GPa) in all considered scenarios (Table 1) has $0.009 \leq T_c/T_F \leq 0.108$ and falls in unconventional superconductors band of the Uemura plot [27,28] (Fig. 2).

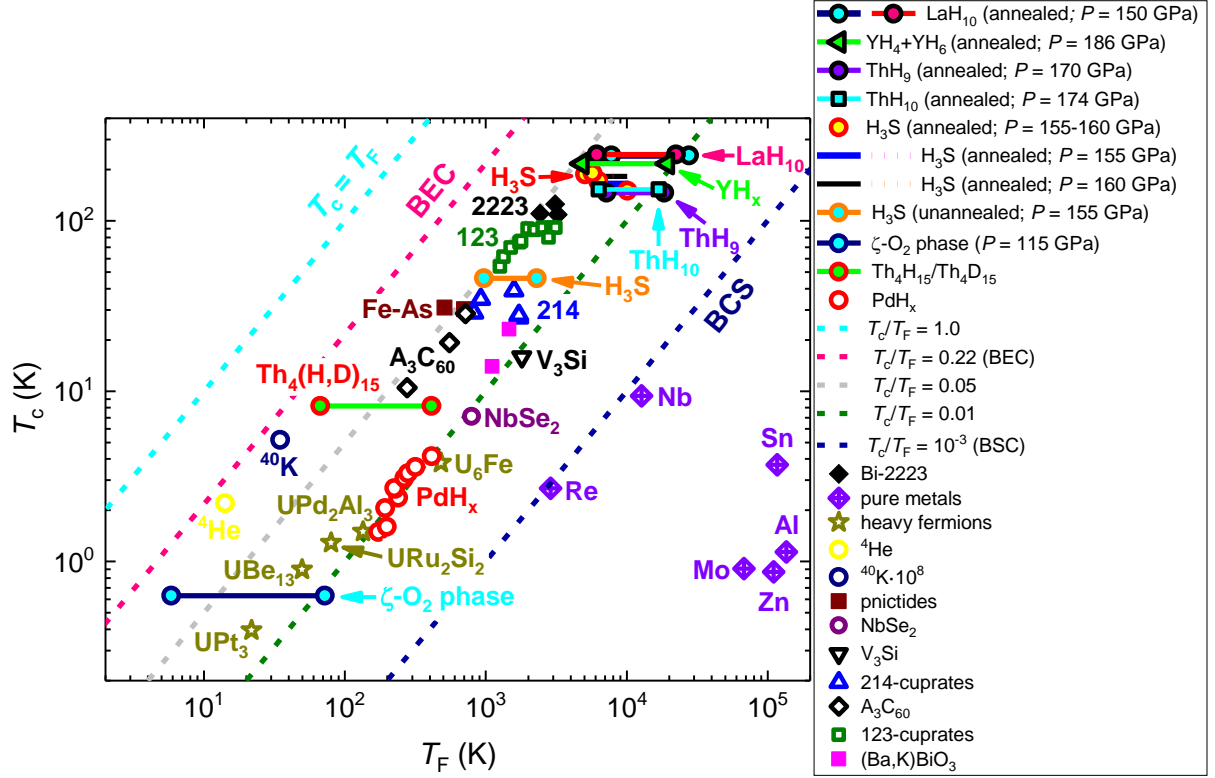


Figure 2. A plot of T_c versus T_F where ζ -O₂ phase compressed at pressure of $P = 115$ GPa is shown together with the most representative superconducting families. Raw data is taken from [24-28]. Characteristic lines for the Bose-Einstein condensate (BEC), the Bardeen-Cooper-Schrieffer (BCS) superconductors and for $T_c/T_F = 1.0, 0.05, 0.01$ are shown for clarity.

It should be stressed that primary physical reason, that ζ -O₂ phase is classified as unconventional superconductor is belong solid experimental result, that this superconductor exhibits relatively high ground state upper critical field, $B_{c2}(0)$, and relatively low superconducting transition temperature, T_c . Truly, if ζ -O₂ phase will be conventional superconductor similar to Al (which exhibits $T_c/T_F = 8.4 \cdot 10^{-6}$), than in accordance with the expression [25] based on BCS theory [33]:

$$B_{c2} \left(\frac{T}{T_c} = 0 \right) = \frac{\pi \cdot \phi_0 \cdot k_B}{16 \cdot \hbar^2} \cdot m_{eff}^* \cdot \alpha^2 \cdot \left(\frac{T_c}{T_F} \right) \cdot T_c = 2.7 \text{ mT} \quad (6)$$

where for the simplicity we assumed that $m_{eff}^* = 1.0 \cdot m_e$ and $\alpha = \frac{2 \cdot \Delta(0)}{k_B \cdot T_c} = 3.53$ are identical to ones for aluminium. We note, that experimental value for ζ -O₂ phase [8] is:

$$B_{c2} \left(\frac{T}{T_c} = 0.08 \right) = 190 \text{ mT}, \quad (7)$$

which is about two orders of magnitude larger than hypothetical value for a conventional superconductor.

V. Conclusions

In summary, in this paper we analyse experimental $B_{c2}(T)$ data for superconducting ζ -O₂ phase of highly-compressed oxygen ($P = 115$ GPa), reported by Shimizu *et al* [8], and find that in all considered scenarios this highly-compressed ζ -O₂ phase is unconventional superconductor.

Acknowledgement

Author also thanks financial support provided by the state assignment of Minobrnauki of Russia (theme “Pressure” No. AAAA-A18-118020190104-3) and by Act 211 Government of the Russian Federation, contract No. 02.A03.21.0006.

References

- [1] Wittig J 1968 Superconductivity of cerium under pressure *Phys. Rev. Lett.* **21** 1250-1252
- [2] Drozdov A P, Eremets M I, Troyan I A, Ksenofontov V, Shylin S I 2015 Conventional superconductivity at 203 kelvin at high pressures in the sulfur hydride system *Nature* **525** 73-76
- [3] Somayazulu M, Ahart M, Mishra A K, Geballe Z M, Baldini M, Meng Y, Struzhkin V V and R. J. Hemley R J 2019 Evidence for superconductivity above 260 K in lanthanum superhydride at megabar pressures *Phys. Rev. Lett.* **122** 027001
- [4] Drozdov A P, *et al* 2019 Superconductivity at 250 K in lanthanum hydride under high pressures *Nature* **569** 528-531
- [5] Struzhkin V V, Hemley R J, Mao H-K and Timofeev Y A 1997 Superconductivity at 10-17 K in compressed sulphur *Nature* **390** 382-384

- [8] Shimizu K, Suhara K, Ikumo M, Eremets M I and Amaya K 1998 Superconductivity in oxygen *Nature* **393** 767-769
- [9] Eremets M I, Trojan I A, Medvedev S A, Tse J S, Yao Y 2008 Superconductivity in hydrogen dominant materials: Silane *Science* 319 1506-1509
- [10] Drozdov A P, Eremets M I, Troyan I A 2015 Superconductivity above 100 K in PH₃ at high pressures *arXiv*:1508.06224
- [11] Troyan I A, *et al.* 2019 Synthesis and superconductivity of yttrium hexahydride *Im $\bar{3}m$ -YH₆* *arXiv*:1908.01534
- [12] Kong P P, *et al.* 2019 Superconductivity up to 243 K in yttrium hydrides under high pressure *arXiv*:1909.10482
- [13] Semenov D V, Kvashnin A G, Ivanova A G, Svitlyk V, Fominski V Yu, Sadakov A V, Sobolevskiy O A, Pudalov V M, Troyan I A and Oganov A R 2019 *Materials Today*, in press DOI: 10.1016/j.mattod.2019.10.005
- [14] Gor'kov L P and Kresin V Z 2018 *Colloquium: High pressure and road to room temperature superconductivity* *Rev. Mod. Phys.* **90** 011001
- [15] Shimizu K 2018 Superconducting elements under high pressure *Physica C* **552** 30-33
- [16] Wang H, Li X, Gao G, Li Y and Ma Y 2018 Hydrogen-rich superconductors at high pressures *WIREs Comput Mol Sci* **8** e1330 (doi: 10.1002/wcms.1330)
- [17] Pickett W and Eremets M I 2019 The quest for room-temperature superconductivity in hydrides *Physics today* **72** 52-58
- [18] Flores-Livas J A, Boeri L, Sanna A, Profeta G, Arita R, Eremets M 2019 A perspective on conventional high-temperature superconductors at high pressure: Methods and materials *arXiv*:1905.06693
- [19] Desgreniers S, Vohra Y K, Ruoff A L 1990 Optical response of very high density solid oxygen to 132 GPa *J. Phys. Chem.* **94** 1117-1122
- [20] Akahama Y, Kawamura H, Häusermann D, Hanfland M and Shimomura O 1995 New high-pressure structural transition of oxygen at 96 GPa associated with metallization in a molecular solid *Phys. Rev. Lett.* **74** 4690
- [21] Serra S, Chiarotti G, Scandolo S and Tosatti E 1998 *Physical Review Letters* **80** 5160-5163
- [22] Weck G, Desgreniers S, Loubeyre P and Mezouar M 2009 *Physical Review Letters* **102** 255503
- [23] Craco L, Laad M S and Leoni S 2017 Microscopic description of insulator-metal transition in high-pressure oxygen *Scientific Reports* **7** 2632
- [24] Talantsev E F 2019 Classifying superconductivity in compressed H₃S *Modern Physics Letters B* **33** 1950195
- [25] Talantsev E F 2019 Classifying hydrogen-rich superconductors *Materials Research Express* **6** 106002
- [26] Talantsev E F and Maitra R C 2020 Classifying superconductivity in ThH-ThD superhydrides/superdeuterides *Materials Research Express* **7**, in press (<https://doi.org/10.1088/2053-1591/ab6770>)
- [27] Uemura Y J 2004 Condensation, excitation, pairing, and superfluid density in high-T_c superconductors: the magnetic resonance mode as a roton analogue and a possible spin-mediated pairing *J. Phys.: Condens. Matter* **16** S4515-S4540
- [28] Uemura Y J 2019 Dynamic superconductivity responses in photoexcited optical conductivity and Nernst effect *Phys. Rev. Materials* **3** 104801
- [29] Baumgartner T, Eisterer M, Weber H W, Fluekiger R, Scheuerlein C, Bottura L 2014 Effects of neutron irradiation on pinning force scaling in state-of-the-art Nb₃Sn wires *Supercond. Sci. Technol.* **27** 015005

- [30] Werthamer N R, Helfand E and Hohenberg P C 1966 Temperature and purity dependence of the superconducting critical field, H_{c2} . III. Electron spin and spin-orbit effects *Phys. Rev.* **147** 295-302
- [31] Gor'kov L P 1960 The critical supercooling field in superconductivity theory *Soviet Physics JETP* **10** 593-599
- [32] Talantsev E F 2019 Classifying induced superconductivity in atomically thin Dirac-cone materials *Condens. Matter* **4** 83
- [33] Bardeen J, Cooper L N, Schrieffer J R 1957 Theory of superconductivity *Phys. Rev.* **108** 1175-1204
- [34] Bambakidis G, Smith R J, and Otterson D A 1968 Electrical resistivity as a function of deuterium concentration in palladium NASA Report Number TN D-4970
- [35] Poole P P, Farach H A, Creswick R J, Prozorov R 2007 Superconductivity (2-nd Edition, London, UK)
- [36] Medvedeva J E 2007 Averaging of the electron effective mass in multicomponent transparent conducting oxides *EPL* **78** 57004
- [37] Kostrzewa M, Szczesniak K M, Durajski A P, Szczesniak R 2019 From LaH₁₀ to room-temperature superconductors arXiv:1905.12308
- [38] Nicol E J and Carbotte J P 2015 Comparison of pressurized sulfur hydride with conventional superconductors *Phys. Rev. B* **91** 220507(R)
- [39] Errea I *et al* 2015 High-pressure hydrogen sulfide from first principles: A strongly anharmonic phonon-mediated superconductor *Phys. Rev. Lett.* **114** 157004
- [40] Durajski A P 2016 Quantitative analysis of nonadiabatic effects in dense H₃S and PH₃ superconductors *Scientific Reports* **6** 38570
- [41] Talantsev E F, Crump W P, Storey J G, Tallon J L 2017 London penetration depth and thermal fluctuations in the sulphur hydride 203 K superconductor *Annalen der Physics* **529** 1600390
- [42] Kaplan D and Imry Y 2018 High-temperature superconductivity using a model of hydrogen bonds *Proc. Nat. Acad. Sci.* **115** 5709-5713